

## Article

# A Supersensitive Method for Spectroscopic Diagnostics of Electrostatic Waves in Magnetized Plasmas

Eugene Oks<sup>1,\*</sup>, Elisabeth Dalimier<sup>2,3</sup> and Paulo Angelo<sup>2,3</sup><sup>1</sup> Physics Department, Auburn University, 380 Duncan Drive, Auburn, AL 36849, USA<sup>2</sup> Laboratoire Pour L'utilisation des Lasers Intenses, Sorbonne Université, CEDEX 05, F-75252 Paris, France; elisabeth.dalimier@upmc.fr (E.D.); paulo.angelo@upmc.fr (P.A.)<sup>3</sup> Centre National de la Recherche Scientifique, Ecole Polytechnique, CEA—Université Paris-Saclay, CEDEX 05, F-75252 Paris, France

\* Correspondence: goks@physics.auburn.edu

**Abstract:** For relatively strong magnetic fields, hydrogen atoms can have delocalized bound states of almost macroscopic dimensions. Therefore, such states are characterized by a Giant Electric Dipole Moment (GEDM), thus making them very sensitive to an external electric field. We considered the manifestations of the GEDM states in hydrogen spectral line profiles in the presence of a quasimonochromatic electrostatic wave of a frequency  $\omega$  in a plasma. We demonstrated that in this situation, hydrogen spectral lines can exhibit quasi-satellites, which are the envelopes of Blochinzew-type satellites. We showed that the *distinctive feature* of such quasi-satellites is that their peak intensity is located at the same distance from the line center (in the frequency scale) for all hydrogen spectral lines, the distance being significantly greater than the wave frequency  $\omega$ . At the absence of the GEDM (and for relatively strong electrostatic waves), the maxima of the satellite envelopes would be at different distances from the line center for different hydrogen lines. We demonstrated that this effect would constitute a *supersensitive diagnostic method* for measuring the amplitude of electrostatic waves in plasmas down to  $\sim 10$  V/cm or even lower.

**Keywords:** strong magnetic fields; center-of-mass effects; giant electric dipole moments; supersensitive diagnostics of electrostatic waves in plasmas



**Citation:** Oks, E.; Dalimier, E.; Angelo, P. A Supersensitive Method for Spectroscopic Diagnostics of Electrostatic Waves in Magnetized Plasmas. *Plasma* **2021**, *4*, 780–788. <https://doi.org/10.3390/plasma4040040>

Academic Editor:  
Andrey Starikovskiy

Received: 19 November 2021  
Accepted: 6 December 2021  
Published: 10 December 2021

**Publisher's Note:** MDPI stays neutral with regard to jurisdictional claims in published maps and institutional affiliations.



**Copyright:** © 2021 by the authors. Licensee MDPI, Basel, Switzerland. This article is an open access article distributed under the terms and conditions of the Creative Commons Attribution (CC BY) license (<https://creativecommons.org/licenses/by/4.0/>).

## 1. Introduction

There are numerous methods for spectroscopic diagnostics of plasmas (see, e.g., books [1–11] listed in chronological order). Among these methods are those designed for spectroscopic diagnostics of various electrostatic waves in plasmas (see, e.g., books [3,10,11]). These methods, based on the shape of spectral lines of atoms and ions, cover the range of amplitudes of the electrostatic waves from  $\sim 1$  kV/cm to  $\sim 1$  GV/cm. In the present paper we describe a possibility to extend the sensitivity of such methods to  $\sim 10$  V/cm or even lower, as follows.

There are plenty of studies showing that for hydrogenic atoms/ions in a uniform magnetic field, the center-of-mass motion and the relative (internal) motion are coupled by the magnetic field and, rigorously speaking, cannot be separated (see, e.g., papers [12–14] and references therein). A pseudoseparation is possible for hydrogen atoms. It leads to a Hamiltonian for the relative motion that depends on a center-of-mass integral of the motion  $\mathbf{K}$  called pseudomomentum but does not depend on the center-of-mass coordinate [14]. We remind that the pseudomomentum  $\mathbf{K}$  is the canonical variable conjugated to the center-of-mass coordinate.

A diamagnetic potential term in the Hamiltonian for the relative motion is responsible for the formation of an additional potential well far away from the hydrogen nucleus (proton). For relatively strong magnetic fields, the new bound states inside this well are delocalized states of almost macroscopic dimensions. Therefore, the bound state inside this

well is characterized by a Giant Electric Dipole Moment (GEDM), thus making such states very sensitive to an external electric field.

In the present paper we consider the effect of a quasimonochromatic electrostatic wave of a frequency  $\omega$  in a plasma on hydrogen spectral lines in the presence of the GEDM states. We show that, in this situation, hydrogen spectral lines can exhibit quasi-satellites. The quasi-satellites are envelopes of Blochinzew-type satellites [15], the latter being separated from the line center by multiples of the wave frequency  $\omega$  (in the frequency scale) in both the red and blue wings. We demonstrated that the *distinctive feature* of such quasi-satellites (in the presence of the GEDM states) is that their peak intensity is located at the same distance from the line center (in the frequency scale) for all hydrogen spectral lines, the distance being significantly greater than the wave frequency  $\omega$ . We showed that this effect would allow measuring the amplitude of electrostatic waves in plasmas down to  $\sim 10$  V/cm or even lower. We provided an example for the conditions of edge plasmas of tokamaks.

### 2. Materials and Methods

We used the analytical method for finding roots of a cubic polynomial, and no materials were used.

### 3. Results

In the Hamiltonian of the relative (internal) motion for the hydrogen atom in a magnetic field  $\mathbf{B}$ , the potential energy has the form (see, e.g., Schmelcher–Cederbaum paper [16], Equation (6))

$$V = [e^2/(2Mc^2)]\mathbf{B} \times \mathbf{r} - [ |e|/(Mc)](\mathbf{B} \times \mathbf{K})\mathbf{r} - e^2/r, \tag{1}$$

where  $\mathbf{K}$  is the pseudomomentum,  $M$  is the mass of the hydrogen atom,  $c$  is the speed of light, and  $e$  is the electron charge. We followed paper [16] in choosing  $e < 0$ ; we also note that in paper [16] it was set at  $c = 1$ . In Equation (1),  $(\mathbf{B} \times \mathbf{K})\mathbf{r}$  stands for the scalar product (also known as the dot-product) of vector  $\mathbf{r}$  and vector  $(\mathbf{B} \times \mathbf{K})$ .

We also assumed the same configuration as chosen in paper [16]:  $\mathbf{B} = (0, 0, B)$  and  $\mathbf{K} = (0, K, 0)$ , where  $K > 0$ . Then, Equation (1) takes the form:

$$V = [e^2B^2/(2Mc^2)](x^2 + y^2) + [ |e|BK/(Mc)]x - e^2/(x^2 + y^2 + z^2)^{1/2}. \tag{2}$$

For simplifying equations, we introduce the following scaled potential energy  $V_s$ :

$$V_s = Mc^2V/(e^2B^2). \tag{3}$$

Then, Equation (2) can be rewritten as follows:

$$V_s = (x^2 + y^2)/2 + [Kc/( |e| B)]x - Mc^2/[B^2(x^2 + y^2 + z^2)^{1/2}]. \tag{4}$$

By equating partial derivatives of  $v_s$  with respect to  $y$  and  $z$  to zeros, we found that this occurred at  $y = z = 0$  (as in paper [16]). The partial derivative of  $v_s$  with respect to  $x$  that we calculated for finding extrema of the potential had the form:

$$\partial V_s/\partial x = x + Kc/( |e| B) + Mc^2x/[B^2(x^2 + y^2 + z^2)^{3/2}]. \tag{5}$$

At  $y = z = 0$ , Equation (5) becomes:

$$\partial V_s/\partial x = x + Kc/( |e| B) + (Mc^2/B^2) (\text{sign } x)/x^2. \tag{6}$$

We remind that  $\text{sign } x = 1$  for  $x > 0$  or  $\text{sign } x = -1$  for  $x < 0$ .

On equating  $\partial V_s/\partial x$  from Equation (6) to zero, we arrived at the following equation:

$$x^3 + [Kc/( |e| B)]x^2 + (Mc^2/B^2)(\text{sign } x) = 0. \tag{7}$$

Thus, for  $x > 0$  and for  $x < 0$ , Equation (7) leads to two different equations.

For  $x > 0$ , Equation (7) becomes:

$$x^3 + [Kc/(|e|B)]x^2 + (Mc^2/B^2) = 0. \tag{8}$$

Obviously, Equation (8) does not have positive roots.

For  $x < 0$ , Equation (7) leads to

$$|x|^3 - [Kc/(|e|B)]|x|^2 + (Mc^2/B^2) = 0. \tag{9}$$

Equation (9) is equivalent to Equation (8b) from paper [16]; we remind that in paper [16] it was set to  $c = 1$  and  $e = -1$ .

The polynomial in Equation (9) has either two or zero real roots. Thus, the total number of roots of Equation (7) is also either two or zero since there are no positive roots.

We note in passing that the authors of paper [16] erroneously stated that  $\partial V/\partial x$ , calculated at  $y = z = 0$ , can have three real roots. Their error originates from the fact that they missed the factor (sign  $x$ ) in the corresponding equation.

We introduce the scaled magnetic field  $b$  and the scaled pseudomomentum  $k$ , as follows

$$b = B/(cM^{1/2}), k = K/(|e|M^{1/2}), \tag{10}$$

where  $b$  has the dimension of  $cm^{-3/2}$  and  $k$  has the dimension of  $cm^{-1/2}$ . Below, while using particular numerical values of  $b$  and  $k$ , we omit the dimensions for brevity.

With these notations, Equation (9) simplifies as follows:

$$|x|^3 - (k/b)|x|^2 + 1/b^2 = 0. \tag{11}$$

The discriminant  $\Delta$  of this cubic equation is

$$\Delta = (4k^3 - 27b)/b^5. \tag{12}$$

Therefore, Equation (11) has two distinct real negative roots if  $\Delta > 0$ , i.e., if

$$k > 3(b/4)^{1/3}. \tag{13}$$

The exact analytical results for the two real roots  $x_1$  and  $x_2$  of Equation (11) are as follows:

$$x_1 = -k/(3b) - (1 + 31/2i) k^2 / \{22/33b [27b - 2k^3 + 33/2(27b^2 - 4k^3b)^{1/2}]^{1/3} - (1 - 31/2i) [27b - 2k^3 + 33/2(27b^2 - 4k^3b)^{1/2}]^{1/3} / (21/36b). \tag{14}$$

$$x_2 = -k/(3b) - (1 - 3^{1/2}i) k^2 / \{2^{2/3}3b[27b - 2k^3 + 3^{3/2}(27b^2 - 4k^3b)^{1/2}]^{1/3} - (1 + 3^{1/2}i) [27b - 2k^3 + 3^{3/2}(27b^2 - 4k^3b)^{1/2}]^{1/3} / (2^{1/3}6b). \tag{15}$$

It should be emphasized that, despite the presence of the imaginary unit  $i$  in Equations (14) and (15), they yield real numbers for  $x_1$  and  $x_2$  under the condition (13).

Figure 1 shows the plot of the root  $x_1$  (solid line) and  $x_2$  (dashed line) versus the scaled magnetic field  $b$  for the scaled pseudomomentum  $k = 10$  (corresponding to  $K = 0.031$  a.u. =  $6.2 \times 10^{-21}$  g cm/s). It is seen that the largest (by the absolute value) root is  $x_1$ .

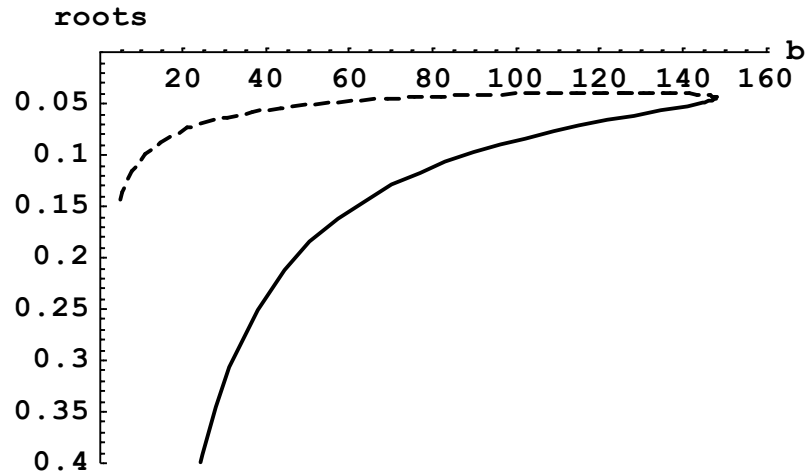
It is easy to find out that, at  $x = x_1$ , one has  $\partial^2 V_s / \partial x^2 > 0$ , so that the scaled potential energy vs. has a minimum at  $x = x_1$  (under condition (13)). At  $x = x_2$  one has  $\partial^2 V_s / \partial x^2 < 0$ , so that the scaled potential energy vs. has a maximum at  $x = x_2$  (under condition (13)).

The scaled potential energy vs. at  $y = z = 0$  has the form:

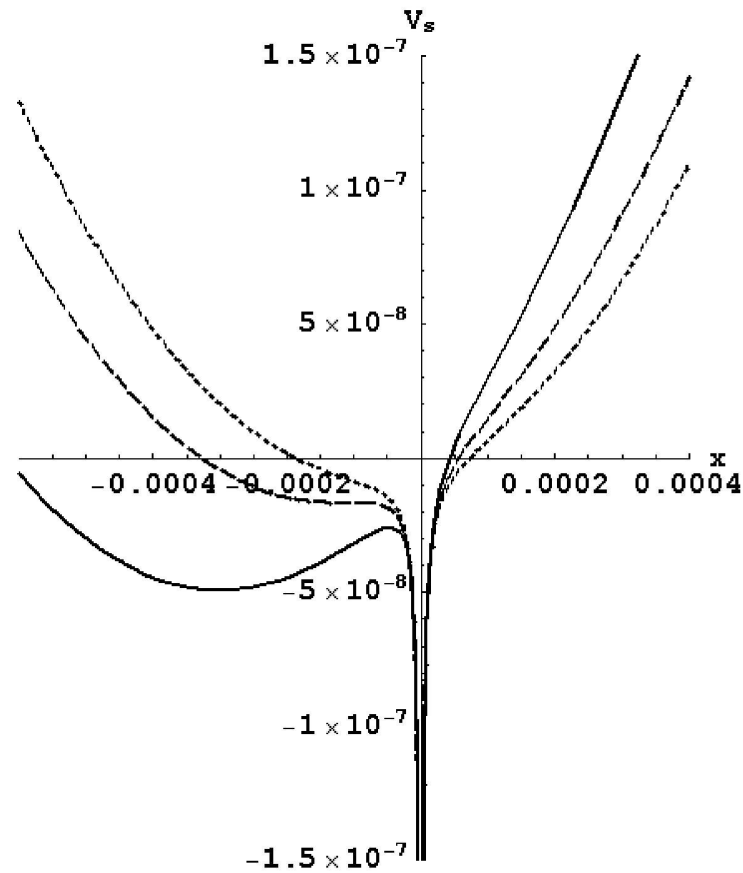
$$V_s = x^2/2 + kx/b - 1/(b^2|x|). \tag{16}$$

Figure 2 shows the plot of the scaled potential energy vs. from Equation (16) versus the coordinate  $x$  (in cm) at the scaled magnetic field  $b = 1.3 \times 10^6$  (corresponding to  $B = 5$  Tesla) for the following three values of the scaled pseudomomentum:  $k = 400$  corresponding to

$K = 1.25$  a.u. (solid line),  $k = 206$  corresponding to  $K = 0.64$  a.u. (dashed line), and  $k = 100$  corresponding to  $K = 0.31$  a.u. (dotted line). These three values of  $k$  correspond to the values of the discriminant in Equation (12)  $\Delta > 0$ ,  $\Delta = 0$ , and  $\Delta < 0$ , respectively. It is seen that for  $k = 400$ , the plot shows a maximum and minimum at  $x < 0$ ; for  $k = 206$ , the plot exhibits a flat part caused by the merging of the maximum and minimum; for  $k = 100$ , the plot does not have any extrema, all of this being consistent with the above analytical results.



**Figure 1.** Plot of the root  $x_1$  (solid line) and  $x_2$  (dashed line) of Equation (11) versus the scaled magnetic field  $b$  for the scaled pseudomomentum  $k = 10$ . The vertical scale is in cm.



**Figure 2.** The scaled potential energy vs. from Equation (16) versus the coordinate  $x$  (cm) at the scaled magnetic field  $b = 1.3 \times 10^6$  (corresponding to  $B = 5$  Tesla) for the following three values of the scaled pseudomomentum:  $k = 400$  corresponding to  $K = 1.25$  a.u. (solid line),  $k = 206$  corresponding to  $K = 0.64$  a.u. (dashed line), and  $k = 100$  corresponding to  $K = 0.31$  a.u. (dotted line).

Figure 3 presents the dependence of the location of the additional potential well  $x_1$  (in cm) on the scaled magnetic field  $b$  and on the scaled pseudomomentum  $k$  in some ranges of these two parameters. It is seen that  $|x_1|$  can reach “macroscopic” values, resulting in a GEDM of such state.

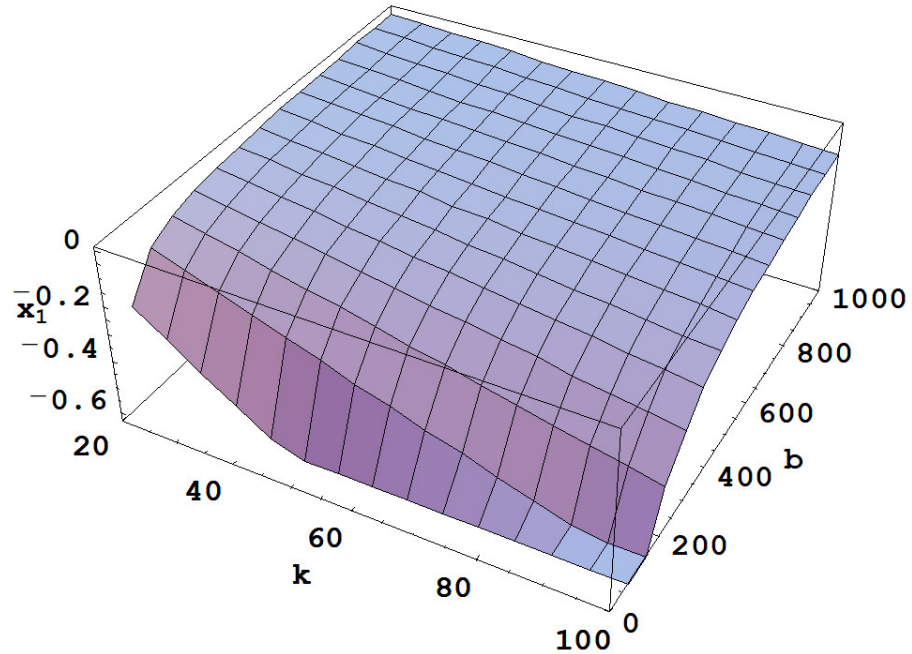


Figure 3. Dependence of the location of the additional potential well  $x_1$  (in cm) on the scaled magnetic field  $b$  and on the scaled pseudomomentum  $k$ .

Schmelcher and Cederbaum, in their paper [16], gave only the following approximate formula for  $x_1$  (converted below into our notations):

$$x_{1,CS} = -k/b + k/(k^3 - 2b). \tag{17}$$

As an example, Figure 4 presents the ratio of the approximate root  $x_{1,CS}$  from paper [16] to the exact root  $x_1$  for the scaled pseudomomentum  $k = 20$ . It is seen that, for a given  $k$ , the relative error of the approximate Formula (17) from paper [16] grows bigger as the scaled magnetic field  $b$  increases.

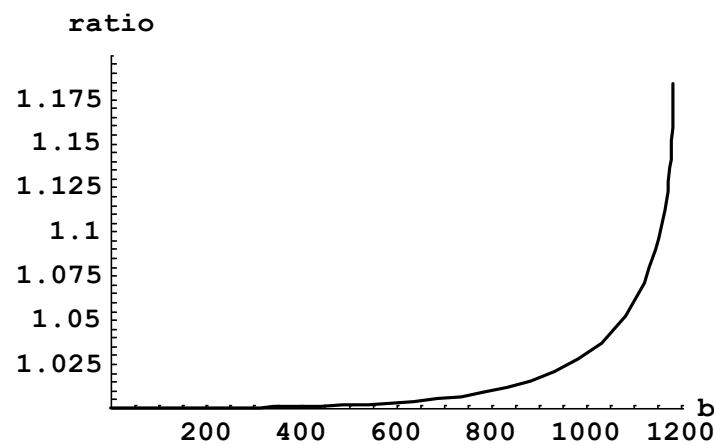
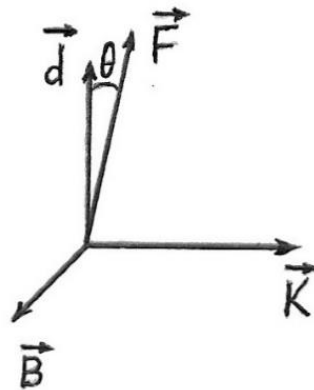


Figure 4. The ratio of the approximate root  $x_{1,CS}$  from paper [16] (reproduced in Equation (17)) to the exact root  $x_1$  for the scaled pseudomomentum  $k = 20$ .

Now let us discuss the corresponding profiles  $S(w)$  of hydrogen spectral lines in a magnetized plasma containing an electrostatic wave  $F\cos\omega t$  that propagates perpendicularly to the magnetic field  $\mathbf{B}$ . Here,

$$w = \Delta\omega/\omega \tag{18}$$

is the scaled detuning from the unperturbed position of the spectral line. Figure 5 presents the orientation of the wave amplitude vector  $\mathbf{F}$  with respect to the magnetic field  $\mathbf{B}$ , the pseudomomentum  $\mathbf{K}$ , and the giant dipole moment  $\mathbf{d}$ , the latter corresponding to the state within the additional potential well located at  $x_1 < 0$ , where  $x_1$  is given by Equation (14).



**Figure 5.** The orientation of the amplitude vector  $\mathbf{F}$  of an electrostatic wave in a magnetized plasma with respect to the magnetic field  $\mathbf{B}$ , the pseudomomentum  $\mathbf{K}$ , and the giant dipole moment  $\mathbf{d}$ , the latter corresponding to the state within the additional potential well located at  $x_1 < 0$ , where  $x_1$  is given by Equation (14).

Under the action of the field  $F\cos\omega t$ , any atomic state possessing a permanent electric dipole moment  $\mathbf{D}$  manifests in the spectral line profile as a series of Blokhinzew-type satellites at the distances  $q\omega$  ( $q = \pm 1, \pm 2, \pm 3, \dots$ ) from the line center (see, e.g., paper [15] and Chapter 3 in book [3]). The actual number of observed satellites depends, first of all, on the so-called modulation parameter

$$\varepsilon = \mathbf{DF}/(\hbar\omega), \tag{19}$$

where  $\mathbf{DF}$  stands for the scalar product (also known as the dot-product) of these two vectors. If  $\varepsilon \ll 1$ , then, at best, practically only the satellites at  $\pm\omega$  might be observed (though not necessarily observed if the spectral line broadening by other mechanisms is relatively large). However, in the case of the GEDM states (the states within the additional potential well) there would be practically always  $\varepsilon \gg 1$ . This situation corresponds to the multi-satellite regime where there would be numerous satellites of significant intensities: The satellites of the maximum intensity would be at  $\Delta\omega \sim \pm\varepsilon\omega$ . In this case, even if the spectral line broadening by other mechanisms is relatively large, one could observe the envelope of multiple satellites (rather than individual satellites), the maximum intensity of the envelope being at  $\Delta\omega \sim \pm\varepsilon\omega$ . More details and more precise formulas are presented in Chapter 3 of book [3].

Let us denote by  $g$  the share of hydrogen atoms that are in the GEDM states (the states within the additional potential well). We consider the case of a relatively weak electrostatic wave in a plasma, so that for hydrogen atoms that are not in the GEDM state, the corresponding modulation parameter from Equation (19) is much smaller than unity. This means that for the share  $(1 - g)$  of hydrogen atoms, the would be satellites are extremely weak and practically do not affect spectral line profiles (e.g., for  $\varepsilon \sim 10^{-3}$ , the relative intensity of the “strongest” satellites would be  $\sim 10^{-6}$ ). Then, the total spectral line profile can be represented in the form

$$S(w) = (1 - g) S_0(w) + gS_1(w), \tag{20}$$

where

$$S_1(w) = \sum J_p^2(\epsilon_1) S_0(w - p), \quad \epsilon_1 = e |x_0| (F \cos\theta) / (\hbar\omega), \quad (21)$$

In Equation (21),  $J_p(\epsilon_1)$  is the Bessel functions and  $e$  is the electron charge. As for the function  $S_0(w)$  in Equations (20) and (21), it is the shape of the spectral line that would be at the absence of the electrostatic wave. It combines in the standard way the Doppler broadening and the Stark broadening by plasma ions and electrons, as well as the Zeeman effect (see, e.g., books [4,10]).

Below, as an example, we consider the situation where the electrostatic wave in a plasma is the upper hybrid wave propagating perpendicularly to the magnetic field  $\mathbf{B}$ . Its well-known frequency is (see, e.g., book [17]):

$$\omega = (\omega_{ce}^2 + \omega_{pe}^2)^{1/2}. \quad (22)$$

Here

$$\omega_{ce} = eB / (m_e c) = 1.76 \times 10^{11} B(\text{Tesla}), \quad (23)$$

is the electron cyclotron frequency ( $c$  being the speed of light) and

$$\omega_{pe} = (4\pi e^2 N_e / m_e)^{1/2} = 5.64 \times 10^4 [N_e(\text{cm}^{-3})]^{1/2} \quad (24)$$

is the plasma electron frequency, where  $N_e$  is the electron density.

For simplicity of formulas, we consider the situation where  $\omega_{ce} \gg \omega_{pe}$ , which is the case if

$$B \gg B_{cr}(\text{Tesla}) = 3.21 \times 10^{-7} [N_e(\text{cm}^{-3})]^{1/2}. \quad (25)$$

In this case, the upper hybrid wave frequency  $\omega$  reduces practically to the electron cyclotron frequency  $\omega_{ce}$ .

As an example, Figure 6 shows the total profiles  $S(\Delta\omega/\omega)$  of the Ly-beta line (solid curve) and the Ly-alpha line (dashed curve) for the case where  $g = 0.25$ , the magnetic field  $B = 5$  Tesla, the plasma temperature  $T = 3$  eV, the electron density  $N_e = 3 \times 10^{13} \text{ cm}^{-3}$ , the pseudomomentum  $K = 2.5 \times 10^{-19} \text{ g cm/s} = 1.25$  at. units, and the projection of the amplitude vector of the upper hybrid wave on the giant dipole moment is  $F \cos\theta = 10 \text{ V/cm}$ . In this case,  $|x_0| = 3.0 \times 10^{-4} \text{ cm} = 5.7 \times 10^4$  at. units and  $\epsilon = 6$ . We note that  $B = 5$  Tesla,  $T = 3$  eV, and  $N_e = 3 \times 10^{13} \text{ cm}^{-3}$  can correspond to the conditions of edge plasmas of tokamaks. The profiles  $S(\Delta\omega/\omega)$  are area-normalized to unity.

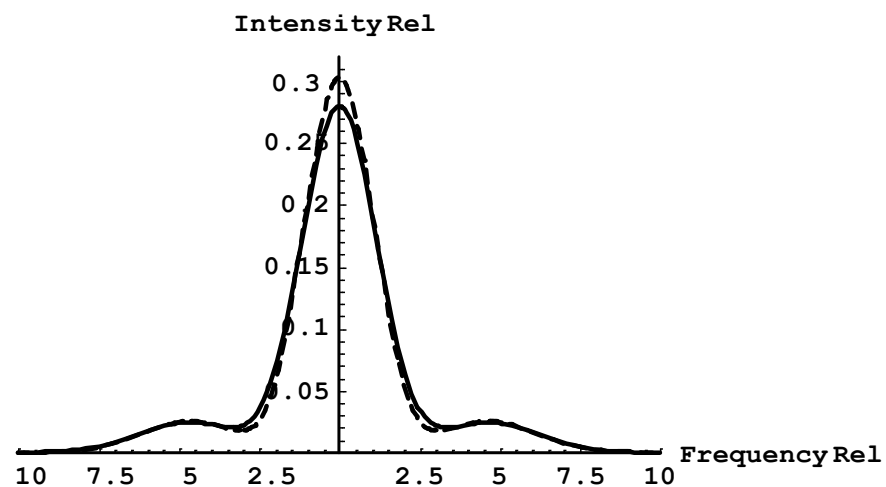


**Figure 6.** Total profiles of the Ly-beta line (solid curve) and the Ly-alpha line (dashed curve) for the case where  $g = 0.25$ , the magnetic field  $B = 5$  Tesla, the plasma temperature  $T = 3$  eV, the pseudomomentum  $K = 2.5 \times 10^{-19} \text{ g cm/s} = 1.25$  at. units, and the projection of the amplitude vector of the upper hybrid wave on the giant electric dipole moment is  $F \cos\theta = 10 \text{ V/cm}$ . The profiles  $S(\Delta\omega/\omega)$  are area-normalized to unity.

It is seen that the *quasi-satellites*, i.e., the maxima of the envelope of multiple satellites, are located at the same distance (in the frequency scale) from the line center for both spectral lines, this distance being significantly greater than the wave frequency.

Actually, *this is true for any two hydrogen lines*. This is the *distinctive feature* of the situation where a share of hydrogen atoms is in the GEDM states. Indeed, if there were not such states and the wave amplitude were large enough for having significant intensities of multiple Blokhinzew-type satellites, the maxima of the satellite envelopes would be at different distances from the line center for different hydrogen lines (see, e.g., book [3], Chapter 3).

In other words, if one would observe quasi-satellites (at the distance from the line center  $\Delta\omega \gg \omega$ ) in the experimental profile of just one hydrogen line, then both of the above interpretations would be possible. However, if one would observe the quasi-satellites at the same distance from the line center  $\Delta\omega \gg \omega$  in the experimental profiles of any two hydrogen lines, then the only possible interpretation would be as follows. First, it would be the manifestation of the presence of the GEDM states of hydrogen atoms. Second, this would constitute a supersensitive method for spectroscopic diagnostics of electrostatic waves in magnetized plasmas, namely, the waves of the amplitude as low as  $\sim 10$  V/cm or even lower.

#### 4. Discussion

We considered how the GEDM states manifest in the profiles of hydrogen spectral lines in the presence of a quasimonochromatic electrostatic wave of a frequency  $\omega$  in a plasma. We demonstrated that, in this situation, hydrogen spectral lines can exhibit quasi-satellites, which are the envelopes of Blokhinzew-type satellites.

We showed that the *distinctive feature* of such quasi-satellites is that their peak intensity is located at the same distance from the line center (in the frequency scale) for all hydrogen spectral lines, the distance being significantly greater than the wave frequency  $\omega$ . At the absence of the GEDM (and for relatively strong electrostatic waves), the maxima of the satellite envelopes would be at different distances from the line center for different hydrogen lines.

We demonstrated that this effect would constitute a *supersensitive diagnostic method*. It would allow measuring the amplitude of electrostatic waves in plasmas down to  $\sim 10$  V/cm or even lower. The observation of satellites of two spectral lines in a series should be feasible since the satellites were observed by various experimental groups at different plasma sources for a variety of the electron densities and temperatures (see, e.g., books [3,10,11] where the corresponding experiments were covered).

Finally, we note that this method would not work for diagnosing stochastic quasimonochromatic waves in plasmas. This is because the maximum of the intensity of the envelope of the satellites, caused by such waves, is at the unperturbed wavelength of the spectral line (rather than being shifted to the wings) (see, e.g., paper [18] and Section 3.2.1 of the book [3]).

**Author Contributions:** Conceptualization, E.O.; investigation, E.O., E.D., P.A.; writing—original draft preparation, E.O., E.D.; writing—review and editing, E.O., E.D. All authors have read and agreed to the published version of the manuscript.

**Funding:** This research received no external funding.

**Data Availability Statement:** All data is included in the paper.

**Conflicts of Interest:** The authors declare no conflict of interest.

#### References

1. Griem, H.R. *Plasma Spectroscopy*; McGraw-Hill: New York, NY, USA, 1964.
2. Griem, H.R. *Spectral Line Broadening by Plasmas*; Academic: New York, NY, USA, 1974.
3. Oks, E. *Plasma Spectroscopy. The Influence of Microwave and Laser Fields*; Springer: New York, NY, USA, 1995.
4. Griem, H.R. *Principles of Plasma Spectroscopy*; Cambridge University Press: Cambridge, MA, USA, 1997.

5. Fujimoto, T. *Plasma Spectroscopy*; Clarendon: Oxford, UK, 2004.
6. Oks, E. *Stark Broadening of Hydrogen and Hydrogenlike Spectral Lines in Plasmas: The Physical Insight*; Alpha Science International: Oxford, UK, 2006.
7. Fujimoto, T.; Iwamae, A. *Plasma Polarization Spectroscopy*; Springer: Berlin, Germany, 2008.
8. Ochkin, V.N. *Spectroscopy of Low Temperature Plasma*; Wiley: Weinheim, Germany, 2009.
9. Kunze, H.-J. *Introduction to Plasma Spectroscopy*; Springer: Berlin, Germany, 2009.
10. Oks, E. *Diagnostics of Laboratory and Astrophysical Plasmas Using Spectral Lines of One-, Two-, and Three-Electron Systems*; World Scientific: Hackensack, NJ, USA, 2017.
11. Oks, E. *Advances in X-Ray Spectroscopy of Laser Plasmas*; IOP Publishing: Bristol, UK, 2020.
12. Schmelcher, P.; Cederbaum, L.S. Classical self-ionization of fast atomic ions in magnetic fields. *Phys. Rev. Lett.* **1995**, *74*, 662. [[CrossRef](#)] [[PubMed](#)]
13. Schmelcher, P.; Cederbaum, L.S. Intermittent chaos in Hamiltonian systems: The three-dimensional hydrogen atom in magnetic fields. *Phys. Rev. A* **1993**, *47*, 2634. [[CrossRef](#)]
14. Vincke, M.; Baye, D. Centre-of-mass effects on the hydrogen atom in a magnetic field. *J. Phys. B At. Mol. Opt. Phys.* **1988**, *21*, 2407. [[CrossRef](#)]
15. Blochinzew, D.I. Zur Theorie des Starkeffektes im Zeitveränderlichen Feld. *Phys. Z. Sov. Union* **1933**, *4*, 501–515.
16. Schmelcher, P.; Cederbaum, L.S. Two-body effects of the hydrogen atom in crossed electric and magnetic fields. *Chem. Phys. Lett.* **1993**, *208*, 548–554. [[CrossRef](#)]
17. Swanson, D.G. *Plasma Waves*; Academic Press: Cambridge, MA, USA, 2012.
18. Lifshitz, E.V. Stark effect in high frequency stochastic fields in a plasma. *Sov. J. Exp. Theor. Phys.* **1968**, *26*, 570.